DOI:
10.1016/j.colsurfb.2018.06.009

Document Version
Peer reviewed version

Activity enhancement of selective antitumoral selenodiazoles formulated with poloxamine micelles

Amaia Úriz[1,2], Carmen Sanmartín*[2,3], Daniel Plano[2,3], Cécile A. Dreiss*[4] and Gustavo González-Gaitano*[1]

[1] University of Navarra, Faculty of Sciences, Department of Chemistry, Irunlarrea 1, E-31008, Pamplona, Spain.
[2] University of Navarra, Faculty of Pharmacy and Nutrition, Department of Organic and Pharmaceutical Chemistry, Irunlarrea 1, E-31008, Pamplona, Spain.
[3] Instituto de Investigación Sanitaria de Navarra (IdiSNA), Irunlarrea 3, E-31008 Pamplona, Spain.
[4] King's College London, Institute of Pharmaceutical Sience, School of Cancer and Pharmaceutical Sciences, Franklin-Wilkins Building, 150 Stamford Street, SE1 9NH London, UK

ABSTRACT: Selenium (Se) incorporated into organic frameworks has demonstrated anticancer activity against several cancer types. One of the drawbacks of most of these constructs is their poor solubility and bioavailability, which can be overcome with the use of suitable nanocarriers. We have synthesized a series of 5-substituted amide selenodiazoles, based on the parent structure of ebselen, an organoselenium drug with proven cytoprotective activity, and solubilized them in polymeric micelles of poloxamines, poly(ethylene oxide)-poly(propylene oxide) X-shaped tetrablock-copolymers. Scattering methods (SANS and DLS) were employed to characterize the micellar nanocarriers. MTT biological evaluation highlights the selectivity of the Se-compounds towards cancer cells, with MCF-7 standing as the most responsive line. The alkylation of the heterocycle with a 12-carbon hydrophobic tail displays the highest activity, showing a 100-fold increase with respect to ebselen. This compound also exhibits the greatest increase in solubility in poloxamine micelles, overall resulting in a one-fold increase in activity with respect to the non-formulated form, making it a hit compound for further optimization.

STATISTICAL SUMMARY: 5365 words (including references), 3 tables, 1 scheme, 4 figures/sub-figures

Activity enhancement of selective antitumoral selenodiazoles formulated with poloxamine micelles

Amaia Úriz[1,2], Carmen Sanmartín*[2,3], Daniel Plano[2,3], Cécile A. Dreiss*[4] and Gustavo González-Gaitano*[1]

[1] University of Navarra, Faculty of Sciences, Department of Chemistry, Irunlarrea 1, E-31008, Pamplona, Spain. [2] University of Navarra, Faculty of Pharmacy and Nutrition, Department of Organic and Pharmaceutical Chemistry, Irunlarrea 1, E-31008, Pamplona, Spain.[3] Instituto de Investigación Sanitaria de Navarra (IdiSNA), Irunlarrea 3, E-31008 Pamplona, Spain. [4] King's College London, Institute of Pharmaceutical Sience, School of Cancer and Pharmaceutical Sciences, Franklin-Wilkins Building, 150 Stamford Street, SE1 9NH London, UK

KEYWORDS selenium, ebselen, polymeric micelles, Tetronics, poloxamines

ABSTRACT: Selenium (Se) incorporated into organic frameworks has demonstrated anticancer activity against several cancer types. One of the drawbacks of most of these constructs is their poor solubility and bioavailability, which can be overcome with the use of suitable nanocarriers. We have synthesized a series of 5-substituted amide selenodiazoles, based on the parent structure of ebselen, an organoselenium drug with proven cytoprotective activity, and solubilized them in polymeric micelles of poloxamines, poly(ethylene oxide)-poly(propylene oxide) X-shaped tetrablock-copolymers. Scattering methods (SANS and DLS) were employed to characterize the micellar nanocarriers. MTT biological evaluation highlights the selectivity of the Se-compounds towards cancer cells, with MCF-7 standing as the most responsive line. The alkylation of the heterocycle with a 12-carbon hydrophobic tail displays the highest activity, showing a 100-fold increase with respect to ebselen. This compound also exhibits the greatest increase in solubility in poloxamine micelles, overall resulting in a one-fold increase in activity with respect to the non-formulated form, making it a hit compound for further optimization.

1. Introduction

Selenium (Se) is a micronutrient for humans; low plasma levels have been linked to a high incidence of several cancers[1,2,3,4]. Nevertheless, outcomes from the SELECT trial (Selenium and Vitamin E Cancer Prevention Trial) have given rise to some controversy about this relationship[5]. One of the main weaknesses of this trial was the chemical form used to deliver selenium (namely, *L*-selenomethionine). This alone could explain the unexpected failure of the SELECT trial since it is well documented that Se speciation is critical for its biological effects[6,7,8]. Indeed, some Se derivatives can be metabolized to form selenocysteine, a Se amino acid that can be incorporated into 25 different selenoproteins. Most of the selenoproteins play essential roles in human health and low levels have been reported in several diseases [9,10,11,12]. At the same time, other Se derivatives can be metabolized to methylselenol (CH_3SeH) or to hydrogen selenide (H_2Se); both present antitumor activities, different than those from selenoproteins[6]. The activity of Se derivatives occurs through several mechanisms, some of them are not fully understood to date[13]. Taking into account all these considerations, it is clear that the activity of Se is dependent on the specific constructs in which it is incorporated, and the failure of some Se compounds should not be generalized to all Se derivatives. Recently, our group and many others have demonstrated that the incorporation of Se into organic frameworks, in particular small molecules such as selenocyanate, diselenide, selenourea or selenide, confers unique and very valuable properties against a range of diseases[14,15], and demonstrate anticancer activity against different cancer types[16,17,18]. Among these small Se-containing molecules, Se heterocycles have demonstrated low toxicity for healthy cells, along with promising anticancer effects. Ebselen is one of the most well studied Se heterocyclic compounds in cancer[19,20].

One of the limitations of most Se-based drugs however is their poor solubility and bioavailability, which can be overcome with the use of suitable nanocarriers[21]. Polymeric micelles based on polyethylene oxide (PEO) and polypropylene oxide (PPO) are emerging as promising nanocarriers, displaying a large array of architectures and properties, in addition to displaying biological inhibitory activity towards drug efflux transporters of the ATP-binding cassette[22,23]. Tetronic® is the trade name of BASF for poloxamines, a family of X-shaped amphiphilic copolymers based on PEO and PPO. Each of the four arms comprises a PEO and a PPO block, which are connected by a central ethylene diamine group. This morphology drives self-assembly into micelles with a lipophilic core (PPO blocks) and a hydrophilic outer shell (PEO blocks), which is highly hydrated. The number of PO and EO units forming the arms varies, affording a range of molecular weights and hydrophilic-lipophilic balance (HLB), and consequently a rich phase behavior and properties[24,25,26]. If the configuration of the blocks is inverted, the resulting amphiphile is called a "reverse" poloxamine (Tetronic-R). The core of the aggregates offers a non-polar environment for the encapsulation of hydrophobic, poorly water-soluble drugs, while the protonable amino connector affords pH-responsiveness of the central moiety and thus controllable release of the cargo.

Within this framework, we have synthesized a family of selenodiazole derivatives bearing a hydrocarbon chain of variable

length (from 3 to 12 carbon atoms, SE3-SE12). This selenodiazole skeleton was chosen based on its similarity with ebselen (also known as PZ51, DR3305, or SPI-1005), and our previous experience on the antitumor and leishmanicidal in vitro activity of selenodiazole derivatives substituted on 5-position with different amides[27,28]. The synthetic strategy to obtain selenodiazole derivatives is outlined in Scheme 1.

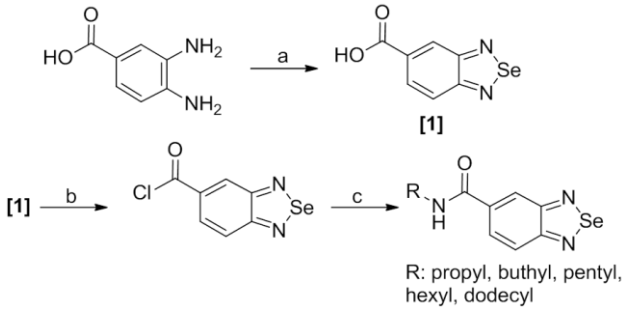

Scheme 1. Synthesis pathway for compounds SE3, SE4, SE5, SE6 and SE12. a) SeO_2, 260 °C, solid phase, 1h. b) $SOCl_2$, reflux, 2h. c) R-NH_2 (R: propyl (SE3), butyl (SE4), pentyl (SE5), hexyl (SE6), dodecyl (SE12)), $CHCl_3$, TEA, r.t., 48h.

These selenocompounds were formulated with two selected poloxamines, T904 (15 EO, 17 PO per arm, *Mw* 6,700) and T1107 (60 EO, 20 PO per arm, *Mw* 15,000), and their combinations with T90R4, which presents a "reverse" structure compared to T904, bearing its PPO blocks on the outer parts of the four arms. T904 and T1107 were chosen according to their different HLB (12-18 and 18-23, respectively) and capacity of T1107 to form gels, thus widening the scope of formulations to injectable thermogels. The combined use of the reverse poloxamine in the mixed micelles is based on the hypothesis that the incorporation of a hydrophobic amphiphile, which, on its own does not aggregate into micelles, can lead to an enhanced hydrophobic locus within the nanoaggregates and, consequently, a higher solubilization capacity of the selenocompounds. Although there are numerous routes of administration for chemotherapeutic drugs, *i.e.* intramuscular, intra-arterial or intrathecal among other, and ideally oral, the vast majority of these drugs are administered intravenously (i.v.), which would be the preferred route of administration for the new derivatives presented here. In this framework, the poloxamine micelles could help to overcome future issues in the pre-clinical development of selenodiazoles.

2. Materials and methods

2.1. Synthesis of the selenocompounds

Compounds derived from benzo[*c*][1,2,5]selenodiazole were synthesized in the solid phase by cyclization of 3,4-diaminobenzoic acid with SeO_2 at high temperature and constant stirring. The product is reacted with an excess of thionyl chloride under reflux conditions, yielding chlorination of the acid. The formation of the amide derivative follows a nucleophilic acyl substitution in the presence of triethylamine. Final products account for amides with a linear 3- (SE3), 4- (SE4), 5- (SE5), 6- (SE6) and 12- (SE12) carbon chain (see SI for details of the synthesis and compound characterization).

Analytical thin-layer chromatography (TLC) was conducted on E. Merck silica gel 60 F254 plates, 250 µm thickness and detection at 254 nm. Compounds were purified by chromatographic column using the solvent mixtures specified in each case. Infrared (IR) spectra were registered using a Thermo Nicolet FTIR Nexus Euro spectrometer with OMNIC 6.0 software. Products are obtained as solids and their spectra were recorded using transmission KBr pellets. Organic elementary analysis (CHN) was made in a LECO CHN-900 microprocessor. The error interval admitted for each compound is ± 0.5 %. Melting points were obtained using a Mettler FP82 heating stage and FP80 control unit, with a 5 ºC per minute heating rate. Nuclear magnetic resonance (NMR) spectra were recorded on a Bruker 400 UltrashieldTM spectrometer (1H, 400 MHz; 13C, 100 MHz) at room temperature (r.t.). Chemical shifts (δ) are expressed in parts per million (ppm) and coupling constants (*J*) in hertz (Hz). The following abbreviations are used to describe peak patterns when appropriate: s (singlet), d (doublet), t (triplet), q (quartet), qt (quintet), dd (double doublet), dq (double quartet) and br (broad). Fluorescence spectra were measured (Edinburgh Instruments FLS920 spectrofluorimeter) to find the characteristic wavelengths of excitation and emission of the synthesized compounds in ethanol and water, so as to simulate the core and shell environments of the poloxamine micelles. UV-Vis spectra were recorded (Agilent 8453 diode-array spectrophotometer) to obtain the characteristic molar absorptivity by the Beer-Lambert law in ethanol and water, in the range $5 \cdot 10^{-6}$ M to $3 \cdot 10^{-5}$ M.

The polymeric surfactants, Tetronic 1107 (T1107) and Tetronic 904 (T904) were a gift from BASF, with reported compositions per arm 60 EO and 20 PO for T1107 (average molecular weight 15000 $gmol^{-1}$) and 15 EO and 17 PO for T904 (average molecular weight 6700 $gmol^{-1}$). The "reverse" Tetronic 90R4 (T90R4) was purchased from Sigma-Aldrich (block composition 16 EO and 18PO).

2.2. Characterization of the nanocarriers

2.2.1. Small-Angle Neutron Scattering (SANS)

Mixtures of T904 with T90R4, and T1107 with T90R4 (5, 15, 25% w/w, in ratios of 80% direct Tetronic to 20% reverse Tetronic) were prepared at their natural pH (8.2), pH 3 (diprotonated form) and pH 6 (monoprotonated form). Experiments were carried out on LOQ instrument at the ISIS spallation neutron source (ISIS, Rutherford-Appleton Laboratory, STFC, Didcot, Oxford). LOQ uses incident wavelengths from 2.2 to 10.0 Å, sorted by time-of-flight, with a fixed sample-detector distance of 4.1 m, which provides a range of scattering vectors (q) from 0.009 to 0.29 $Å^{-1}$. The samples were prepared in D_2O (Aldrich, > 99.9% in D) to ensure sufficient contrast between the polymer and the solvent and then placed in clean disc-shaped quartz cells (Hellma) of 1 mm path length, controlling the temperature from 20 to 50°C with an external thermostat. All scattering data were first normalized for sample transmission and then background-corrected using a quartz cell filled with D_2O, and finally corrected for the linearity and efficiency of the detector response using instrument-specific software package. The data were then converted to the differential scattering cross-sections, expressed in absolute units of cm^{-1}, using the standard procedures for LOQ. SANS curves were fitted using SasView 3.1.0 software[29]. Scattering curves from the poloxamines in their unimer form were fitted with a four-arm star-shape (4SP) polymer model, while micelles were fitted to a core-shell sphere (CSS) model combined with a

hard-sphere structure factor (HS). When coexisting in solution, a mixed model of unimers and micelles was used by combining the above two models.

2.2.2. *Phase diagrams*

Aqueous solutions of T904 (1-25% wt%), T1107 (1-25 wt%) and mixtures of T904 with T90R4 as well as T1107 with T90R4 (5-25% wt% total concentration with 80% direct Tetronic/20% reverse Tetronic) were placed into a water bath at an initial temperature of 25 ºC. The samples were gradually heated up by 5 ºC increments up to 80 ºC. All samples were prepared at their natural pH (ca. 8.2), pH 3 and pH 6, by adding the required amount of concentrated HCl.

2.2.3. *Dynamic Light Scattering (DLS)*

Size distributions of the poloxamine in water were obtained with a photon correlation spectrometer Malvern Zetasizer Nano, with a laser wavelength of 633 nm. The samples were filtered prior to the measurements by 0.22 µm Millex syringe PVDF filters onto semi-micro glass cells, and the temperature of the samples controlled with 0.1˚C accuracy by the built-in Peltier in the cell compartment. The viscosity and refractive index of the solvent at different temperatures were taken into account to obtain the particle size distribution from the analysis of the autocorrelation function, which was performed with the Zetasizer software in the high-resolution mode to better distinguish overlapping distributions.

2.2.4. *Solubilization studies*

An excess of compound (SE3, SE6 and SE12) was introduced in vials with 15% w/w solutions of polymer (T904, T1107, T904+T90R4 (80%/20% direct/reverse Tetronic), T1107+T90R4 (80%/20% direct/reverse Tetronic)) or in pure water. Samples were left to stir in the water bath at 40 ºC and measured after 72 and 92 h to assure maximum solubility was reached. Drug concentration was obtained from the absorbance data using each poloxamine system as a blank, and the previously established Beer-Lambert law equation.

2.3. *Cytotoxicity studies*

Synthesized selenodiazoles were tested in vitro against cultured cells of leukaemia (CCRF-CEM), colon (HT-29), lung (HTB-54), prostate (PC-3) and breast (MCF-7) cancer by means of the tetrazolium assay (MTT). All the compounds were also tested for toxicity in a mammary gland cell culture derived from non-malignant cells (184B5). All cells were defrosted and maintained in Dulbecco's modified Eagle's medium (DMEM) supplemented with 10% fetal bovine serum (FBS) and 1% penicillin/streptomycin at 37 ºC and 5% CO_2. 1 mmol of compound was diluted in 1 mL DMSO to a concentration of 10^{-2} M and filtered with 0.22 µm Millipore filter to ensure sterility. Serial dilutions were made using non-supplemented media to achieve concentrations from 10^{-3} to 10^{-7} M. 96-well plates were seeded with 100 µL of cellular suspension (100 cells/ µL), 80 µL of media and 20 µL of compound solution, obtaining final samples of concentration 10^{-4}-10^{-8} M. Each sample was evaluated in quadruplicate measurements and repeated in three independent cell samples. Non-supplemented media was used as a blank and controls were performed for each cell line. The same methodology was followed to test three representative compounds (SE3, SE6, SE12) encapsulated in polymer micelles (T904, T1107 and T904+T90R4 (80%/20% direct/reverse Tetronic)). In this case, samples were prepared in 15% (w/w) poloxamine and dilutions performed to obtain samples at 10^{-3} to 10^{-7} M, following the previously described protocol. Blanks were made with each poloxamine system.

3. Results and discussion

3.1. *Structural characterization of the nanocarriers*

Analysis of phase diagrams (SI, Tables S1A and S1B) shows that the most hydrophilic T1107 forms a gel at around 35 ºC and 25%, while the requirements for T904 to form gel are more extreme. In the mixed systems, the incorporation of T90R4 hinders the formation of a gel phase for T904 and shifts the sol-gel transition by 5 ºC for T1107 at 25%T1107.

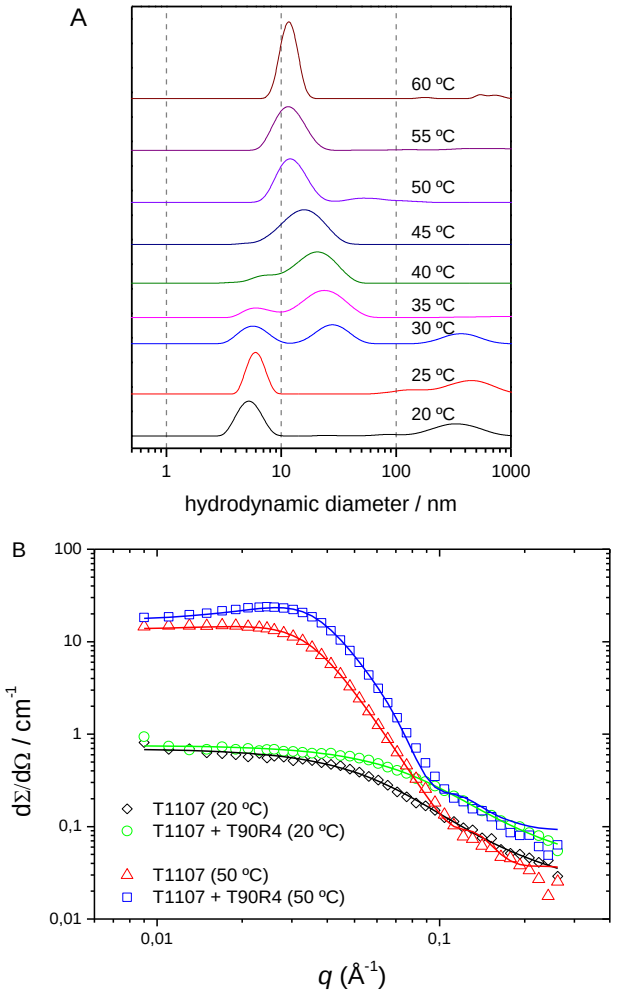

Figure 1. (A) DLS Intensity size distribution for T1107+T90R4 2% (1:1 mass ratio) as a function of temperature. Only unimers are present up to 25 ºC, a mixture of unimers and micelles at intermediate temperatures (30-40 ºC) and only micelles over 40 ºC. (B) SANS curves for the T1107+T90R4 mixture and T1107 alone at 20 and 50 ºC (solid lines are fits to the 4SP and CSS models described in the text)

Precise structural information on the polymeric nanocarriers can be obtained from small-angle neutron scattering (SANS) and dynamic light scattering (DLS). As an example, Figures 1A and 1B show the DLS size distribution and SANS scattering patterns for mixtures of T1107 with the reverse poloxamine as a function of temperature, for 2% of each Tetronic. At 20 ºC, both surfactants are in the form of unimers, and

SANS patterns under these conditions are suitably described by a four-arm-star polymer model (4SP), with an average radius of gyration of 25 Å, matching the hydrodynamic radii observed by DLS. As the temperature increases, upon reaching the critical temperature (CMT), unimers self-organise to form micelles, behaviour typical of PEO-PPO based surfactants[24-26]. At 30ºC a new distribution in the DLS size distribution appears at 30 nm, corresponding to the mixed micelles, although its contribution in mass is still very low. At higher temperature, unimers coexist with the micelles, and the contribution of the peak corresponding to the unimers concomitantly reduces, while the broad peak due to the micelles becomes narrower and shifts to smaller sizes. At 40ºC mixed micelles are fully formed and there is just one peak at ca. 15 nm in size. The solubilization of the reverse poloxamine T90R4 in the micelles is evidenced by a shift of the phase separation, from 36 ºC for T90R4 alone, to ca. 60 ºC when mixed with either T904 or T1107. This effect can be observed in the phase diagrams at a higher direct/reverse Tetronic mass ratio of 4:1 (SI, Table S1A and S1B).

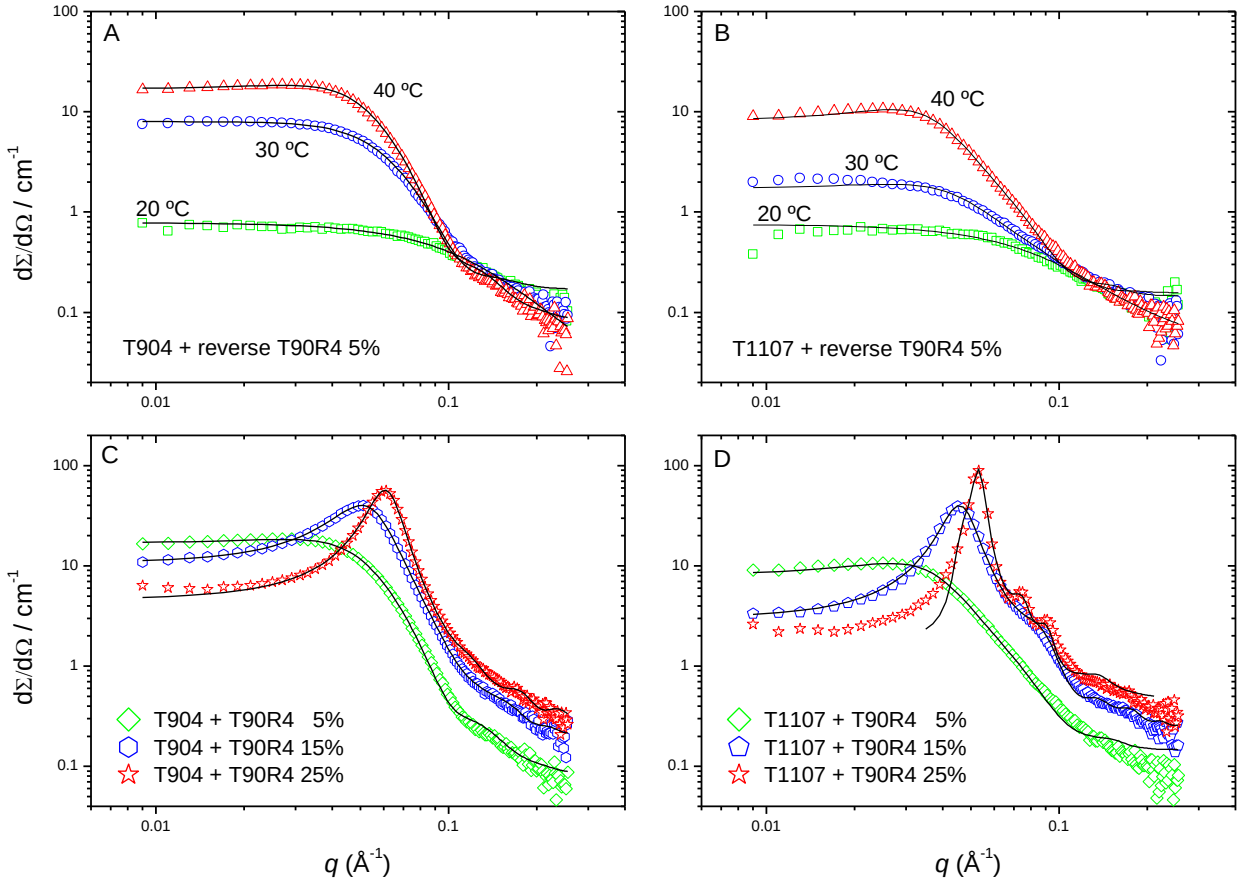

Figure 2. SANS patterns for direct and reverse poloxamine solutions at varying temperatures and concentrations. (A) T904+T90R4 5% as a function of temperature; models used are 4SP (green), 4SP+CSS (blue) and CSS-HS (red). (B) T1107+T90R4 5% as a function of temperature. Models used are: 4SP (green), 4SP+CSS (blue) and CSS-HS (red). (C) T904+T90R4 at 40 ºC, concentrations 5, 15, and 25%, model used is CSS-HS. (D) T1107+T90R4 at 40 ºC, concentrations 5, 15, and 25%; models used are CSS+HS (green, blue) and a body centre cube (bcc) paracrystal (red).

Micelles are appropriately described by a core-shell spherical model (CSS) combined with a hard sphere structure (HS) factor, allowing the estimation of the geometrical parameters and hydration state of micellar core and shell (Figure 2A to C)[24].

The parameters derived from the fits (Table 1) show that substituting a direct unimer by its reverse counterpart does not have a significant impact on the overall size of the micelles. Increasing the polymer concentration, instead, induces a slight shrinkage of the hydrophilic shell. The scattering length density (sld) of the core, which was set as a floating parameter in the fits, reaches values close to the sld of PPO ($3.4 \cdot 10^{-7}$ Å^{-2}), reflecting a dehydrated hydrophobic core (no penetration of solvent). Instead, the sld of the shell tends to that of pure solvent ($6.36 \cdot 10^{-6}$ Å^{-2}), showing a very high extent of hydration of the PEO blocks. It is worth mentioning that the shell sld is lower in all cases than the corresponding value for the pure poloxamine, indicating more permeability to the solvent. At high concentrations, gels are formed (Tables S1A and S1B). Thus, at 25% T1107 + T90R4 (4:1 ratio, 40 ºC), the long-range order responsible for gelation is reflected by a sharp diffraction peak in the 0.07-0.09 Å^{-1} *q*-region (Figure 2D), not observed for T904. The analysis of the SANS data by means of a paracrystal bcc model yields a cell parameter of 167 Å, which matches the dimensions obtained with the same model for T1107 alone. A core size of 35 Å is obtained for the packed micelles, which is very similar to that of the mixed micelles under dilute conditions (Table 1), and to T1107 alone at the same concentration and temperature. The behavior of T904 in combination with 90R4 follows the same trend, as shown in Table 1.

Table 1. Micellar structural parameters at 40 ºC in D_2O obtained from SANS data analysis: *Rc* (core radius), *t* (shell thickness), ϕ (volume fraction from the hard-sphere potential), ρ_s (scattering length density of the shell). In the mixed systems, the concentration is given as the total wt %, at a 4:1 weight ratio.

Polymeric micelles	R_c / Å	*t* / Å	ϕ	$\rho_s \times 10^6$ / Å^{-2}
T904 8%	35	21	0.18	5.87
T904-T90R4 5%	35	26	0.09	6.22
T904-T90R4 15%	35	21	0.27	6.23
T904-T90R4 25%	34	19	0.40	6.20
T1107 5%	34	45	0.18	5.94
T1107-T90R4 5%	34	44	0.11	6.08
T1107-T90R4 15%	33	37	0.39	6.02

In the view of exploiting the pH to control the delivery of the cargo from the micellar core, the effect of pH on the morphology of the aggregates was studied next. Upon a reduction of the pH below the second pK_a (pH 6), the partial protonation of the central ethylene diamine connector leads to a decrease of the scattering. A further reduction below the first pK_a (pH 3) yields curves reminiscent of the unimer form, with radii of gyration similar to those of the respective unimers forming the micelles at its natural pH (pH 8.2), as obtained from fits to a 4SP model. Overall, this means that the protonation of the amino groups causes strong electrostatic repulsion between the direct Tetronic unimers in the core, and the reverse Tetronic in the shell. This destabilizes the mixed micelles, leading first to a mixture of free unimers and aggregates (pH 6), and then to a full rupture of the structures where only unimers are present (pH 3) (SI, Figure S1).

Overall, the structural analysis on the mixed micelles shows that the copolymer with the reverse configuration, largely insoluble on its own, can be incorporated inside the direct micelles. The dimensions of the micelles are not impacted by substituting up to 20% in weight by the reverse structure. The hydrophobic core presents a high degree of packing of the PPO blocks, while the main impact of incorporating the reverse poloxamine is a slight increase of the hydration of the PEO shell. Hence, from a structural viewpoint, any of the combinations is suitable for the solubilization of a hydrophobic cargo.

3.2. Drug Encapsulation

The solubilization of selected organoselenium constructs (SE3, SE6, SE12) was studied in direct poloxamines (T904, T1107) and in their mixtures with the reverse copolymer (T904+T90R4, T1107+T90R4) (Figure 3). As expected, the construct with the shorter alkyl chain, SE3, displays the highest solubility in water at $4.92 \cdot 10^{-4}$ M. Increasing the length of the hydrocarbon tail drastically reduces solubility, with values of $3.5 \cdot 10^{-5}$ M and $9 \cdot 10^{-6}$ M obtained for SE6 and SE12. Incorporation into the polymeric nanocarriers enhances the solubility (Figure 3), with the best solubilization observed with the smaller T904. The addition of the reverse Tetronic T90R4, hypothesized to expand the hydrophobic locus of solubilization, instead slightly reduces the total drug loading. The effect is more pronounced with the long chain organoselenium constructs (SE6 and SE12), whereas for the less hydrophobic compounds (SE3), a slight improvement is noted in the mixed T1107 micelles compared to T1107 alone.

Overall, while the incorporation of the reverse polymer leaves micellar dimensions virtually unchanged, a possible rearrangement of the polymer chains (in particular a more open and hydrated corona) may lead to a different environment, less favorable to drug solubilization, at least for the compounds synthesized here.

3.3. Anticancer activity and selectivity

The drug constructs were evaluated for their cytotoxic activity using MTT assays against a panel of five human tumor cell lines as a representative selection of liquid, solid and hormone-dependent tumors, including lymphocytic leukemia (CCRF-CEM), lung carcinoma (HTB-54), colon carcinoma (HT-29), prostate adenocarcinoma (PC-3) and breast adenocarcinoma (MCF-7) (SI, Figure S2). In order to evaluate the selectivity of the drugs, their toxicity was also assessed against a non-malignant cell line derived from normal breast tissue (184B5). The results are expressed in terms of IC_{50}, the concentration that reduces by 50% the growth of treated cells with respect to untreated controls.

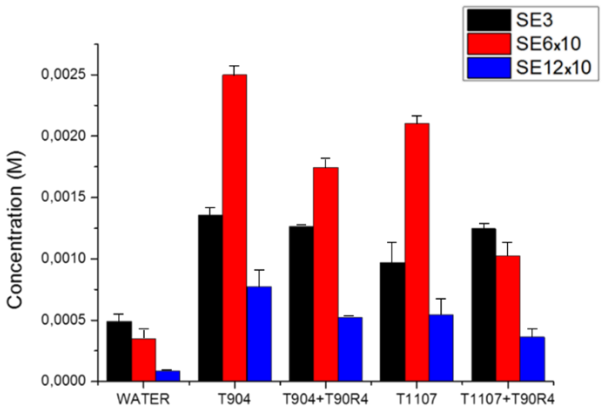

Figure 3. Solubility studies. Final concentration (M) of SE3, SE6 and SE12 after 3 days at 40 ºC in water, T904, T904+T90R4, T1107 and T1107+T90R4. Tetronic concentrations used are 15 % w/w, as for the biological assays. Concentrations of SE6 and SE12 are multiplied by a factor of ten.

SE12 shows a remarkable cytotoxic profile, together with selectivity, under our experimental conditions, with IC_{50} values lower than 1 µM in MCF-7 and PC-3 and higher than 100 µM for 184B5 (Table 2). This represents a 65 and 100-fold increase (for MCF-7 and PC-3, respectively) compared to the reference drug ebselen. These results suggest that the long alkyl lateral chain plays a key role in the activity of the drug, with 12 atoms of carbon being the optimal length. In addition, SE4 and SE12 combine potency and selectivity, a highly attractive feature for anticancer drugs, whose toxic side effects are a limitation to their use.

Table 2. MTT results for leukaemia (CCRF-CEM), colon (HT-29), lung (HTB-54), prostate (PC-3) and breast (MCF-7) cancer cells as well as non-cancer breast tissue cells (184B5).

	IC_{50} / μM					
	CCRF-CEM	HT-29	HTB-54	PC-3	MCF-7	184B5
SE3	91.9	>100	>100	>100	>100	>100
SE4	>100	>100	>100	>100	11.1	>100
SE5	68.4	>100	>100	>100	84.3	>100
SE6	45.7	81.2	>100	84.4	>100	>100
SE12	>100	11.5	>100	0.20	0.90	>100
Ebselen	57.1	>100	68.8	>100	58.8	30.1

In a further step, and since the poor solubility of Se compounds is a limitation to their clinical use, the activity of the constructs was assessed in formulations with the different Tetronics and combinations with the reverse one. MTT assays on the most responsive cell line (MCF-7) were repeated on representative compounds (SE3, SE6 and SE12) encapsulated in T904, T904+T90R4 and T1107 micelles (Figure 4). Table 3 reveals a remarkable decrease of the IC_{50} values for the compounds loaded in T904 and T904+T90R4 mixed micelles in comparison to the non-formulated constructs, particularly noticeable for SE12 (Figure 4), (SI, Figures S3, S4 and S5). While T1107 and T90R4 show some cytotoxicity on their own, T904 has minimum effect on the cells, making it the ideal candidate for the development of delivery systems (SI, Figures S3, S4 and S5).

Considering together the cell growth inhibition, it can be stated that the substitution of the selenodiazole framework in position 5 with aliphatic chains result in an outstanding increase of the anticancer activity for this class of compounds. A comparison of the reported cytotoxic activity for the unsubstituted carboxylic acid ([1] in Scheme 1) and carboxamide[27] with the derivatives presented herein reinforce this molecular design, making it a very promising approach to develop more potent and selective antitumor agents.

To our knowledge, the only Se-containing compound to date modified to form nanocapsules is selol incorporated in a polymeric shell composed of poly(methyl vinyl ether-co-maleic anhydride) (PVM/MA). Nonetheless, this modification yielded only a slight increase in the cytotoxicity in lung cells after 72 h of treatment[30]. Accordingly, the use of poloxamines in selenodiazole derivatives achieved a much higher increase in the antitumor activity, making this construct very promising.

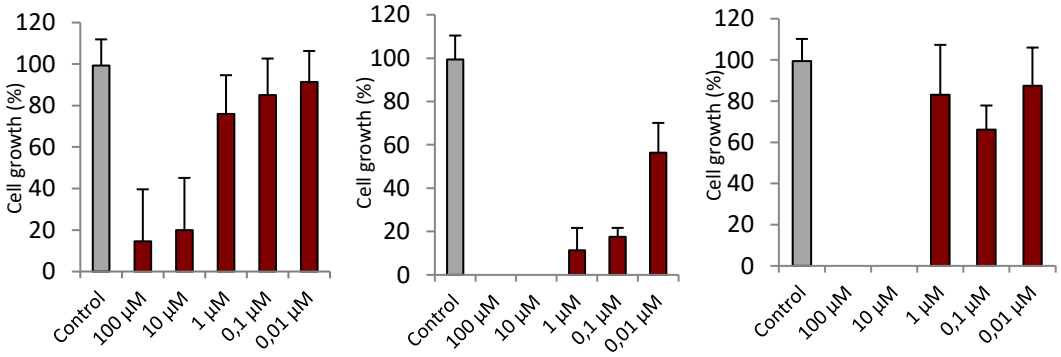

Figure 4. Cytotoxicity results on SE12 encapsulated in Tetronic systems (15% w/w) and tested against breast cancer MCF-7 cell line. From left to right SE12 in T904, in T904+T90R4 and in T1107.

Table 3. IC_{50} values for encapsulated and non-encapsulated selenocompounds SE3, SE6 and SE12. Results obtained by MTT assay performed on MCF-7 cells.

	IC_{50} / μM			
	No encapsulation	T904	T904+T90R4	T1107
SE3	>100	6.20	1.33	46.85
SE6	>100	1.38	0.52	>10
SE12	0.9	0.05	0.03	>1

4. Conclusions

In summary, based on the importance of Se for human health and positive evidence from the literature on Se-heterocycles and in particular the commercial drug ebselen, we have created a small library of selenocompounds, 5-substituted amide selenodiazoles with increasing hydrophobicity, derived from alkyl lateral chains ranging from 3 to 12 carbon atoms. Given the low solubility and poor bioavailability of Se-based compounds being a barrier towards their clinical use, our constructs were encapsulated in PEO-PPO tetrablock copolymer micelles, namely, Tetronics T904 and T1107, and their combination with the reverse copolymer T90R4, which has hydrophobic blocks as end blocks, and is poorly soluble. The incor-

poration of these new constructs within the micelles largely enhanced their solubility, thus offering a route towards higher bioavailability. Combined SANS and DLS studies allowed us to characterize the nanoaggregates as presenting a core-shell morphology, with a dense PPO core and a largely hydrated PEO corona. The largely insoluble reverse Tetronic T90R4 is incorporated within the micelles (up to 20% of the total weight), and, aside from a higher hydration of the corona, does not impact the structural parameters of the micelles, albeit slightly reducing the drug loading within the aggregates. Biological evaluation highlights the selectivity of the constructs towards cancer cells, MCF-7 being the most responsive line. The construct with the longest alkyl side chain, SE12, shows the best activity by far, with up to a 100-fold increase with respect to ebselen. A further improvement of the activity is achieved by encapsulation within the polymeric micelles. The smaller and more hydrophobic T904 displays the highest solubilization capacity, combined to the highest activity enhancement, pointing to the combination of this nanocarrier with SE12 as a promising candidate for further optimization.

5. Acknowledgements

The authors thank ISIS for the provision of beam time and Richard Heenan and Steve King (Rutherford Appleton Laboratory) for their assistance with the SANS experiments. Financial support from projects MAT2014-59116-C2-2-R of the Spanish MINECO, Plan de Investigación de la Universidad de Navarra, PIUNA (Ref 2014–26), and Caixa Foundation-UNED is acknowledged. A.U. is grateful to the School of Science of the UN for the SIP and Erasmus grants for her internship at KCL.

6. References

(1) He, D.; Wang, Z.; Huang, C.; Fang, X.; Chen, D. Serum Selenium Levels and Cervical Cancer: Systematic Review and Meta-Analysis. *Biol. Trace Elem. Res.* **2017**, *179* (2), 195–202.

(2) Zhang, Z.; Bi, M.; Liu, Q.; Yang, J.; Xu, S. Meta-Analysis of the Correlation between Selenium and Incidence of Hepatocellular Carcinoma. *Oncotarget* **2016**, *7* (47).

(3) Shen, F.; Cai, W.-S.; Li, J.-L.; Feng, Z.; Cao, J.; Xu, B. The Association Between Serum Levels of Selenium, Copper, and Magnesium with Thyroid Cancer: A Meta-Analysis. *Biol. Trace Elem. Res.* **2015**, *167* (2), 225–235.

(4) Dunn, B. K.; Richmond, E. S.; Minasian, L. M.; Ryan, A. M.; Ford, L. G. A Nutrient Approach to Prostate Cancer Prevention: The Selenium and Vitamin E Cancer Prevention Trial (SELECT). *Nutr. Cancer* **2010**, *62* (7), 896–918.

(5) Klein, E. A.; Thompson, I. M.; Lippman, S. M.; Goodman, P. J.; Albanes, D.; Taylor, P. R.; Coltman, C. SELECT: The Selenium and Vitamin E Cancer Prevention Trial: Rationale and Design. *Prostate Cancer Prostatic Dis.* **2000**, *3*, 145.

(6) Weekley, C. M.; Harris, H. H. Which Form Is That? The Importance of Selenium Speciation and Metabolism in the Prevention and Treatment of Disease. *Chem. Soc. Rev.* **2013**, *42* (23), 8870.

(7) Vinceti, M.; Grill, P.; Malagoli, C.; Filippini, T.; Storani, S.; Malavolti, M.; Michalke, B. Selenium Speciation in Human Serum and Its Implications for Epidemiologic Research: A Cross-Sectional Study. *J. Trace Elem. Med. Biol.* **2015**, *31*, 1–10.

(8) Wrobel, J. K.; Power, R.; Toborek, M. Biological Activity of Selenium: Revisited. *IUBMB Life* **2016**, *68* (2), 97–105.

(9) Speckmann, B.; Steinbrenner, H. Selenium and Selenoproteins in Inflammatory Bowel Diseases and Experimental Colitis. *Inflamm. Bowel Dis.* **2014**, *20* (6), 1110–1119.

(10) Cardoso, B. R.; Roberts, B. R.; Bush, A. I.; Hare, D. J. Selenium, Selenoproteins and Neurodegenerative Diseases. *Metallomics* **2015**, *7* (8), 1213–1228.

(11) Rose, A. H.; Hoffmann, P. R. Selenoproteins and Cardiovascular Stress. *Thromb. Haemost.* **2015**, *113* (3), 494–504.

(12) Schomburg, L. Selenium, Selenoproteins and the Thyroid Gland: Interactions in Health and Disease. *Nat. Rev. Endocrinol.* **2011**, *8* (3), 160–171.

(13) Rayman, M. P. Selenium in Cancer Prevention: A Review of the Evidence and Mechanism of Action. *Proc. Nutr. Soc.* **2005**, *64* (4), 527–542.

(14) Alcolea, V.; Plano, D.; Karelia, D. N.; Palop, J. A.; Amin, S.; Sanmartin, C.; Sharma, A. K. Novel Seleno- and Thio-Urea Derivatives with Potent in Vitro Activities against Several Cancer Cell Lines. *Eur. J. Med. Chem.* **2016**, *113*, 134–144.

(15) Plano, D.; Karelia, D. N.; Pandey, M. K.; Spallholz, J. E.; Amin, S.; Sharma, A. K. Design, Synthesis, and Biological Evaluation of Novel Selenium (Se-NSAID) Molecules as Anticancer Agents. *J. Med. Chem.* **2016**, *59* (5), 1946–1959.

(16) Diaz-Argelich, N.; Encio, I.; Plano, D.; Fernandes, A. P.; Palop, J. A.; Sanmartin, C. Novel Methylselenoesters as Antiproliferative Agents. *Molecules* **2017**, *22* (8).

(17) Diaz, M.; Gonzalez, R.; Plano, D.; Palop, J. A.; Sanmartin, C.; Encio, I. A Diphenyldiselenide Derivative Induces Autophagy via JNK in HTB-54 Lung Cancer Cells. *J. Cell. Mol. Med.* **2017**.

(18) Alcolea, V.; Plano, D.; Encio, I.; Palop, J. A.; Sharma, A. K.; Sanmartin, C. Chalcogen Containing Heterocyclic Scaffolds: New Hybrids with Antitumoral Activity. *Eur. J. Med. Chem.* **2016**, *123*, 407–418.

(19) Azad, G. K.; Tomar, R. S. Ebselen, a Promising Antioxidant Drug: Mechanisms of Action and Targets of Biological Pathways. *Mol. Biol. Rep.* **2014**, *41* (8), 4865–4879.

(20) Ramakrishnan, N.; Kalinich, J. F.; McClain, D. E. Ebselen Inhibition of Apoptosis by Reduction of Peroxides. *Biochem. Pharmacol.* **1996**, *51* (11), 1443–1451.

(21) Santi, C.; Tidei, C.; Scalera, C.; Piroddi, M.; Galli, F. Selenium Containing Compounds Form Poison to Drug Candidates. *Curr. Chem. Biol.* **2013**, *7* (1), 25–36.

(22) Duncan, R.; Vicent, M. J. Polymer Therapeutics-Prospects for 21st Century: The End of the Beginning. *Adv. Drug Deliv. Rev.* **2013**, *65* (1), 60–70.

(23) Alakhova, D. Y.; Kabanov, A. V. Pluronics and MDR Reversal: An Update. *Mol. Pharm.* **2014**, *11* (8), 2566–2578.

(24) Gonzalez-Gaitano, G.; Muller, C.; Radulescu, A.; Dreiss, C. A. Modulating the Self-Assembly of Amphiphilic X-Shaped Block Copolymers with Cyclodextrins: Structure and Mechanisms. *Langmuir* **2015**, *31* (14), 4096–4105.

(25) Gonzalez-Gaitano, G.; da Silva, M. A.; Radulescu, A.; Dreiss, C. A. Selective Tuning of the Self-Assembly and Gelation of a Hydrophilic Poloxamine by Cyclodextrins. *Langmuir* **2015**, *31* (20), 5645–5655.

(26) Serra-Gomez, R.; Dreiss, C. A.; Gonzalez-Benito, J.; Gonzalez-Gaitano, G. Structure and Rheology of Poloxamine T1107 and Its Nanocomposite Hydrogels with Cyclodextrin-Modified Barium Titanate Nanoparticles. *Langmuir* **2016**, *32* (25), 6398–6408.

(27) Plano, D.; Moreno, E.; Font, M.; Encio, I.; Palop, J. A.; Sanmartin, C. Synthesis and in Vitro Anticancer Activities of Some Selenadiazole Derivatives. *Arch. Pharm. (Weinheim).* **2010**, *343* (11–12), 680–691.

(28) Moreno, D.; Plano, D.; Baquedano, Y.; Jimenez-Ruiz, A.; Palop, J. A.; Sanmartin, C. Antileishmanial Activity of Imidothiocarbamates and Imidoselenocarbamates. *Parasitol. Res.* **2011**, *108* (1), 233–239.

(29) http://www.sasview.org/, Developed by the DANSE Project under NSF Award DMR-0520547.

(30) de Souza L. R.; Muehlmann L. A.; Dos Santos M. S.; Ganassin R.; Simón-Vázquez R.; Joanitti G. A.; Mosiniewicz-Szablewska E.; Suchocki P.; Morais P. C.; González-Fernández A.; Azevedo R. B.; Báo S. N. PVM/MA-shelled Selol Nanocapsules Promote Cell Cycle Arrest in A549 Lung Adenocarcinoma Cells. *J. Nanobiotechnology*. **2014**, *12*, 32.

7. Graphical Abstract

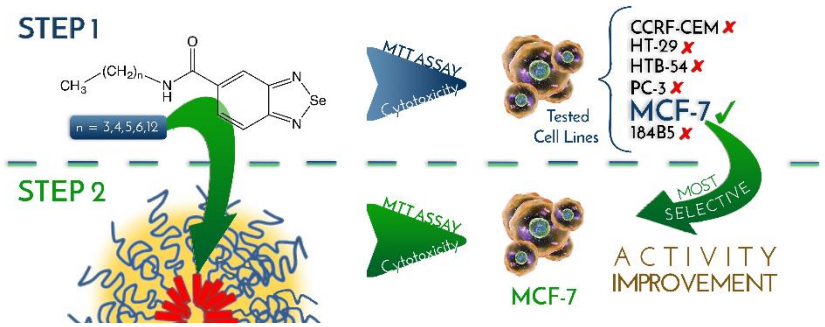

*Author(s), Corresponding Author(s)**

*Gustavo González-Gaitano *[1], Carmen San-martín *[2], and Cécile A. Dreiss *[4]*

Title

Activity enhancement of selective antitumoral selenodiazoles formulated with poloxamine micelles